SHAPE PRIOR INTEGRATED IN AN AUTOMATED 3D REGION GROWING METHOD

J-L. ROSE[1]*, Ch. REVOL-MULLER*[1]*, Mo. ALMAJDUB*[2]*, Em. CHEREUL*[1,2] *,Ch. ODET*[1]

[1]CREATIS, CNRS UMR 5220, Inserm U 630, Université Claude Bernard Lyon1, INSA-Lyon, 69621 Villeurbanne, France
[2]ANIMAGE- Rhône-Alpes GENOPOLE, Bat. CERMEP, 59 Bd Pinel, 69003 Lyon, France

ABSTRACT

We propose a new automated Region Growing method Integrating Shape Prior (RGISP). The aim of this work is to improve region growing segmentation by taking into account a reference model. Our algorithm is assessed on a synthesized image and compared with two other methods in order to point up the contribution of shape prior. It was also applied to segment in-vivo μ-CT images of mouse kidneys in the framework of small animal imaging. RGISP gives promising results and appears to be well adapted to satisfy small animal imaging constraints.

Index Terms— Image processing, image segmentation

1. INTRODUCTION

Segmentation is an important step in medical image processing for feature extraction and quantitative analysis of physiopathologic phenomena. The aim of this process is to retrieve automatically anatomical structures of interest. Since its introduction by Zucker et al. [1], region growing has become a popular method for 3D segmentation. Starting from a seed, manually or automatically located, the iterative process of region growing consists in extracting a region of interest by merging all the neighboring pixels that satisfy some aggregation criterion. This region-based approach relies upon low level features of image such as grey levels of pixels and norms of intensity gradients. Nonetheless, this information is often not sufficient to segment accurately a whole object. Indeed, the performance of region growing is inherently limited, because it is impossible to dissociate connected structures having similar intensities or statistics. To face this problem, additional information must be taken into account during growth such as geometrical constraints or shape prior.

Only few authors integrated geometric prior in region growing. Demeshki et al. [2] compute the shape index of each voxel from an approximation of the boundary of the evolving region. The region growing takes into account the characterization of the topological shape of each voxel. The extracted feature enables separating the desired object from other connected objects that have different shapes but the same intensity value. In the framework of the level set method, shape prior is classicaly represented by a distance map [3, 4] based on signed distance.

In this work, our main contribution is to improve the performance of the region growing approach by taking into account shape information through distance map. This prior information enables a correct segmentation in spite of noise effect or corrupted data. In section 2, we present our 3D region growing method integrating shape prior. In section 3, we test our algorithm on a synthesized image. We analyze the results and point up the contribution of shape prior. In section 4, we present some results of RGISP applied in the framework of a small animal imaging.

2. RGISP METHOD

2.1. Principle of RGISP

The main objective of this work is to integrate global shape information in the process of region growing. This prior knowledge is given by a 3D reference model. Thanks to this reference, it is enabled to assess a geometrical distance between the boundaries of the evolving region and the model. This term is integrated in the process of region growing as a shape prior. Thus, the growing region is attracted by a force near the solution and is not stopped by a possible extremum inside object. As region growing is governed by an aggregation criterion, the resulting segmentation usually depends on the threshold value fixed for this criterion. Within RGISP, the optimal threshold is determined automatically by scanning the decreasing values of the threshold until the mean intensity gradient over the whole boundary of the segmented object is maximized [5] while the mean distance to the reference model is minimized.

2.2. Shape prior

We note I, a 3D image defined on the domain Ω, $x \in \Omega$ a voxel of the image and $I(x)$ the grey level value of x.

Let R^{in} be the evolving region and R^{ref} the reference region. The boundaries of R^{in} and R^{ref} are denoted by Γ and Γ^{ref} respectively. In biomedical imaging, shape prior may stem indifferently from various origins. For example, the reference

contour Γ^{ref} may be initialized from a numerical atlas, it may be either defined interactively by an operator, or deduced from a previous segmentation of a reference image. Nonetheless, we assume in our work that the reference model is already affine registered with the data to segment.
We note $d(x, \Gamma^{ref})$ the signed Euclidean distance between a voxel x and the reference contour Γ^{ref} defined in (1):

$$d(x,\Gamma^{ref}) = \begin{cases} 0 & , \ x \in \Gamma^{ref} \\ -\min\limits_{y\in\Gamma^{ref}} (d(x,y)), & x \in R^{ref} - \Gamma^{ref} \\ +\min\limits_{y\in\Gamma^{ref}} (d(x,y)), & x \in \Omega - R^{ref} \end{cases} \tag{1}$$

where $d(x, y)$ is the Euclidean distance between two voxels x and y. By definition, $d(x, \Gamma^{ref})$ is equal to the signed distance from x to the nearest voxel belonging to the reference boundary. Once and for all, $d(x, \Gamma^{ref})$ is computed for each voxel of the image and stored in a distance map [6]. A negative (resp. positive) value indicates that the voxel is inside (resp. outside) the reference region. In order to be less dependent on the size of the object to segment, the distance map is normalized by the absolute value of the minimum signed distance. In next section, we detail how this shape prior is taken into account in the aggregation criterion.

2.3. Aggregation criterion

The process of growth in RGISP is standard. The merge of a pixel to the evolving region is governed by an aggregation criterion which must be satisfied. At each step, a set of pixels neighboring to the evolving region and also verifying the aggregation criterion, is added to R^{in}, results in a new R^{in} region. The process stops when no more voxels can be added. Let us note $\varphi(x) \in [0, 1]$ the function used for assessing the aggregation criterion for a voxel x. The aggregation criterion is true when:

$$\varphi(x) \geq \delta \tag{2}$$

where $\delta \in [0, 1]$ is a given threshold. In this work, $\varphi(x)$ is computed from two terms $\varphi_{region}(x)$ and $\varphi_{shape}(d(x, \Gamma^{ref}))$ as expressed in (3):

$$\varphi(x) = \varphi_{region}(x) \times \varphi_{shape}\left(d\left(x, \Gamma^{ref}\right)\right) \tag{3}$$

The first term $\varphi_{region}(x) \in [0, 1]$ defined in (4) corresponds to a measure of similarity (or homogeneity) between $I(x)$ and R^{in}. We assume that the underlying distribution of grey levels in R^{in} is approximated by a Gaussian with mean μ and standard deviation σ.

$$\varphi_{region}(x) = \exp^{\frac{-(I(x)-\mu)}{2\sigma^2}} \tag{4}$$

The nearer $I(x)$ is to μ, the nearer $\varphi_{region}(x)$ is to 1. μ and σ are estimated at each step from R^{in}.

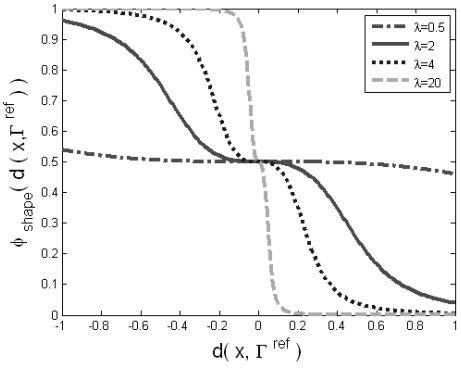

Fig. 1. $\varphi_{shape}(d(x, \Gamma^{ref}))$ for different λ values

Whereas $\varphi_{region}(x) \in [0, 1]$ is driven by image data, the second term $\varphi_{shape}(d(x, \Gamma^{ref}))$ defined in (5) takes into account geometrical features and the proximity of x to the reference model:

$$\varphi_{shape}(d(x,\Gamma^{ref})) = \frac{(\frac{\pi}{2}) - \tan^{-1}((\lambda \times d(x,\Gamma^{ref}))^3}{\pi} \tag{5}$$

where λ is a tuning parameter and $d(x, \Gamma^{ref})$ is the signed Euclidean distance (1). As shown in Figure 1, when $d(x, \Gamma^{ref})$ is negative *i.e.* x inside the reference object, $\varphi_{shape}(d(x, \Gamma^{ref}))$ takes a value close to 1, thus helps the aggregation of x. When $d(x, \Gamma^{ref})$ is positive *i.e.* x outside the reference object, $\varphi_{shape}(d(x, \Gamma^{ref}))$ takes a value close to 0, thus acts against the aggregation of x. When $d(x, \Gamma^{ref})$ is close to 0, *i.e.* x close to the reference contour, $\varphi_{shape}(d(x, \Gamma^{ref}))$ takes a constant value equal to 0.5. The aggregation criterion becomes more selective in the area $\varphi(x) = \varphi_{region}(x)/2$ than inside R^{ref}. For the same threshold δ, a pixel in this area will be added to R^{in} only if $\varphi_{region}(x)$ is twice-higher than for a pixel located inside the object of reference. The width of the flat evolution of $\varphi_{shape}(d(x, \Gamma^{ref}))$ is parameterized by λ value. The lower λ value, the wider the flat area, and the less shape prior is taken into account. When λ is equal to 0, $\varphi_{shape}(d(x, \Gamma^{ref}))$ is equal to 0.5, whatever the value of $d(x, \Gamma^{ref})$. So, the aggregation criterion becomes independent of shape prior and behaves as a simple homogeneity criterion used in the classical region growing. Parameter λ may be related to the accuracy of the prerequisite registration of the reference model with data. The better the registration is, the higher λ can be set.

2.4. Optimal threshold

As mentioned in equation (2), the segmentation obtained by region growing is highly dependent on the choice of δ the threshold which steps in the aggregation criterion. Within RGISP, we propose a solution to automatically find out δ_{opt}

the optimal threshold leading to the best segmentation.
In order to evaluate $Q(\delta)$, the quality of the resulting segmentation obtained with a threshold δ, two features are retained: i) $Q_{image}(\delta)$ based on the mean normalized intensity gradient over the whole boundary of the segmented object noted Γ_δ, and ii) $Q_{shape}(\delta)$ based on the mean Euclidean distance between the pixels belonging to Γ_δ and the reference contour Γ^{ref}.
$Q_{image}(\delta) \in$[0, 1] estimates the contrast along Γ_δ (6). The higher the value of $Q_{image}(\delta)$ is, the more likely Γ_δ matches true edges in the image.

$$Q_{image}(\delta) = \frac{\sum_{x \in \Gamma_\delta} \|\nabla I(x)\|}{Card(\Gamma_\delta)} \quad (6)$$

where $Card(\Gamma_\delta)$ is the number of voxels in the set Γ_δ.
$Q_{shape}(\delta) \in$[0, 1] evaluates the match of Γ_δ with Γ^{ref} (7). The higher the value of $Q_{shape}(\delta)$ is, the better Γ_δ fits Γ^{ref}.

$$Q_{shape}(\delta) = 1 - \frac{\sum_{x \in \Gamma_\delta} \left| d\left(x, \Gamma^{ref}\right) \right|}{Card(\Gamma_\delta)} \quad (7)$$

We define $Q(\delta)$ as the sum of $Q_{image}(\delta)$ and $Q_{shape}(\delta)$:

$$Q(\delta) = Q_{image}(\delta) + Q_{shape}(\delta) \quad (8)$$

The optimal threshold δ_{opt} is determined by the following expression.

$$\delta_{opt} = \underset{\delta \in [0,1]}{\arg\max}\ Q(\delta) \quad (9)$$

Shape prior provided by $Q_{shape}(\delta)$ improves the detection of δ_{opt} by preventing RGISP from converging to a non significant region which could maximize $Q_{image}(\delta)$.

3. EVALUATION AND DISCUSSION

We apply RGISP on a 2D noisy synthesized image Figure 2(b) in order to assess the performance of our method. Figure 2(a) represents the object of interest.
In Figure 2(b), Gaussian noise and corruption were added. So, the different parts of the image are characterized by different Gaussian distributions of grey levels (object: G_o(μ_o=120, σ_o=10); background: G_b(μ_b=80, σ_b=30); anomalous rectangle and inside of the handle: G_a(μ_a=160, σ_a=20). Figure 2(c) displays the reference shape used as shape prior. It is shown that the model differs slightly from the object, since no chip appears at the bottom. Figure 3 shows the results of RGISP for different λ values, i.e. for different degrees of shape prior integration. The white contours delineate segmented regions. The correct detection rates (*cdr*: percent of well classified pixels) are also mentioned bellow each segmentation. In all the cases, the optimal segmentation was found with δ_{opt} = 0.41. For λ=0.5, shape prior is almost not taken into account

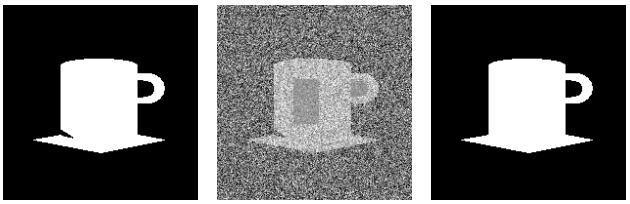

(a) original image (b) noisy image (c) reference model

Fig. 2. Synthesized data: a) object to segment; b) noisy and corrupted synthesized image; c) reference model

in the aggregation criterion, so RGISP fails to segment the object by rejecting sparse pixels inside the object and by aggregating wrong pixels in the hole of the handle. For λ=4, shape prior starts to produce its effects, since topological information of the model can be fully retrieved in the segmented object. For λ=20 and λ=50, RGISP achieves quite good segmentations: pixels in the anomalous rectangle are accepted whereas those in the hole of the handle are rejected. It can be noticed that despite the difference between the reference model and the initial object, RGISP succeeds in retrieving the object with the chip even for a high value of λ.
Moreover, *cdr* values are all bigger than 98% and increase with λ, thus demonstrating the improvement brought by shape prior. Figure 4 compares the segmentation results obtained by three methods: an automated thresholding, RGISP without shape prior (λ=0) and RGISP with λ=50.

It appears that RGISP performs much better than region growing without shape prior with a suppression of 86% misclassified pixels.

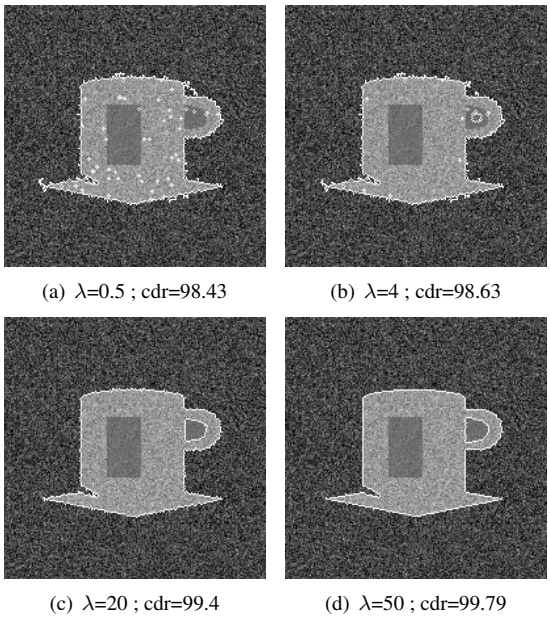

(a) λ=0.5 ; cdr=98.43 (b) λ=4 ; cdr=98.63

(c) λ=20 ; cdr=99.4 (d) λ=50 ; cdr=99.79

Fig. 3. RGISP Segmentations for different λ values

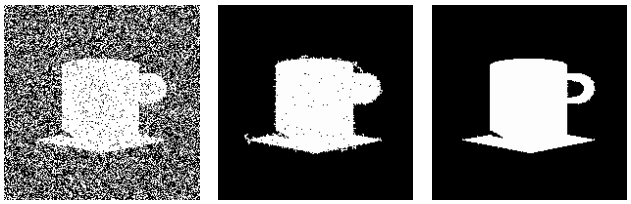

(a) cdr=62 (b) cdr=98.5 (c) cdr=99.79, $\lambda = 50$

Fig. 4. Comparative results: a) automated thesholding, b) RGISP without prior shape, c) RGISP with prior shape

4. APPLICATION ON 3D BIOMEDICAL IMAGES

RGISP was applied in the framework of small animal imaging, provided by the platform Animage. The aim of this application is the phenotyping of the mouse by analysis of kidney volume. We tested RGISP on *in vivo* μ-CT images of kidney of mouse (Balb/c), acquired after injection of an iodized product of contrast. The volume has 240x220x330 8 bits voxels with 35μm isotropic resolution.
The 3D reference model in Figure 5(b) was obtained by a previous segmentation of a reference image (Figure 5(a)). RGISP was tested on a different input image shown in Figure 5(c). The reference model of kidney was previously affine-registered by using ITK library (http://www.itk.org/). RGISP without shape prior fails to segment the kidney due to the strong inhomogeneities (Figure 5(d)) whereas RGISP with $\lambda = 10$ achieves a correct segmentation (Figure 5(e), 5(f)). λ value was set much for the purpose of flexibility with regards to registration and to let the region growing fit data. The compromise is quite satisfying since shape prior allows recovering the object shape more efficiently and introduces a kind of regularization in the region growing process (Figure 5(e)).

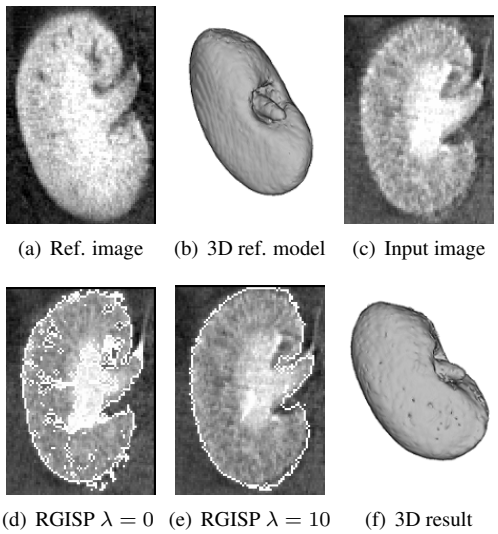

(a) Ref. image (b) 3D ref. model (c) Input image

(d) RGISP $\lambda = 0$ (e) RGISP $\lambda = 10$ (f) 3D result

Fig. 5. μ-CT images of mouse kidney segmented by RGISP

5. CONCLUSION

In this paper, a new method of automated region growing including shape prior is presented. This prior is based on a reference model which may more or less constrain the process of region growing, so that even corrupted objects can be correctly segmented. Through our experimental results, RGISP appears to meet positively the requirements raised by small animal imaging *i.e.* automation and robustness for the analysis of huge data flow generated by longitudinal studies in time.

6. ACKNOWLEDGEMENTS

This work is funded by the EUMORPHIA project (QLG2-CT-2002-00930) which is supported by the European Commission under FP5. The authors wish to thank the Animage platform, Rhône-Alpes Genopole and Fondation Rhône-Alpes Futur funded by the Réseau National des Genopoles.
This work is in the scope of the scientific topics of the PRC-GdR ISIS research group of the French National Center for Scientific Research CNRS.

7. REFERENCES

[1] S. W. Zucker, "Region growing: Childhood and adolescence.," *Computer Graphics and Image Processing*, vol. 5, no. 3, pp. 382–399, 1976.

[2] J. Dehmeshki, X. Ye, and J. Costello, "Shape based region growing using derivatives of 3d medical images: Application to semi-automated detection of pulmonary nodules," in *IEEE ICIP*, 2003, vol. 1, pp. 1085–1088.

[3] M. E. Leventon, W. E. L. Grimson, and O. Faugeras, "Statistical shape influence in geodesic active contours," in *IEEE CVPR*, 2000, vol. 1, pp. 316–323.

[4] A. Tsai, A. Yezzi Jr., W. Wells III, C. Tempany, D. Tucker, A. Fan, W. E. Grimson, and A. Willsky, "Model-based curve evolution technique for image segmentation," in *IEEE CVPR*, 2001, vol. 1, pp. 463–468.

[5] C. Revol-Muller, F. Peyrin, Y. Carrillon, and C. Odet, "Automated 3d region growing algorithm based on an assessment function," *Pattern Recognition Letters*, vol. 23, no. 1-3, pp. 137–150, 2002.

[6] P. E. Danielsson, "Euclidean distance mapping.," *Computer Graphics and Image Processing*, vol. 14, no. 3, pp. 227–248, 1980.